SUPPLEMENTAL INFORMATION

$CRL2^{LRR1}$ targets a CDK inhibitor for cell cycle control in *C. elegans* and actin-based motility regulation in human cells

Natalia G. Starostina, Jennifer Simpliciano, Michael A. McGuirk, and Edward T. Kipreos

SUPPLEMENTAL FIGURES AND TABLES

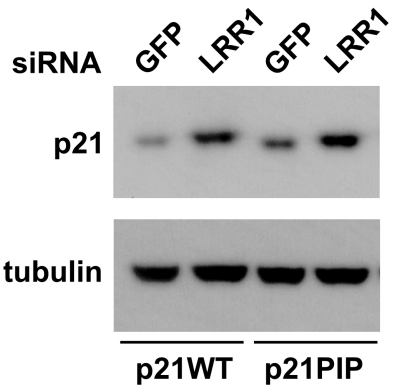

Figure S1, related to Figure 5. LRR1-mediated degradation of p21 does not require the PIP-box motif
HeLa cells were transfected with wild-type p21 (WT) or with PIP-box mutant p21 (PIP), in which the PIP-box sequence of p21 (QTSMTDFY) was substituted with eight alanine residues (Kim et al., 2008), and co-transfected with GFP siRNA (control) or LRR1 siRNA #1. The levels of p21 in the cytoplasmic fractions of the cells were assessed by western blot. Note that in cells treated with LRR1 siRNA, the levels of both wild-type p21 and p21 PIP-box mutant increase to a similar extent compared to the GFP siRNA samples.

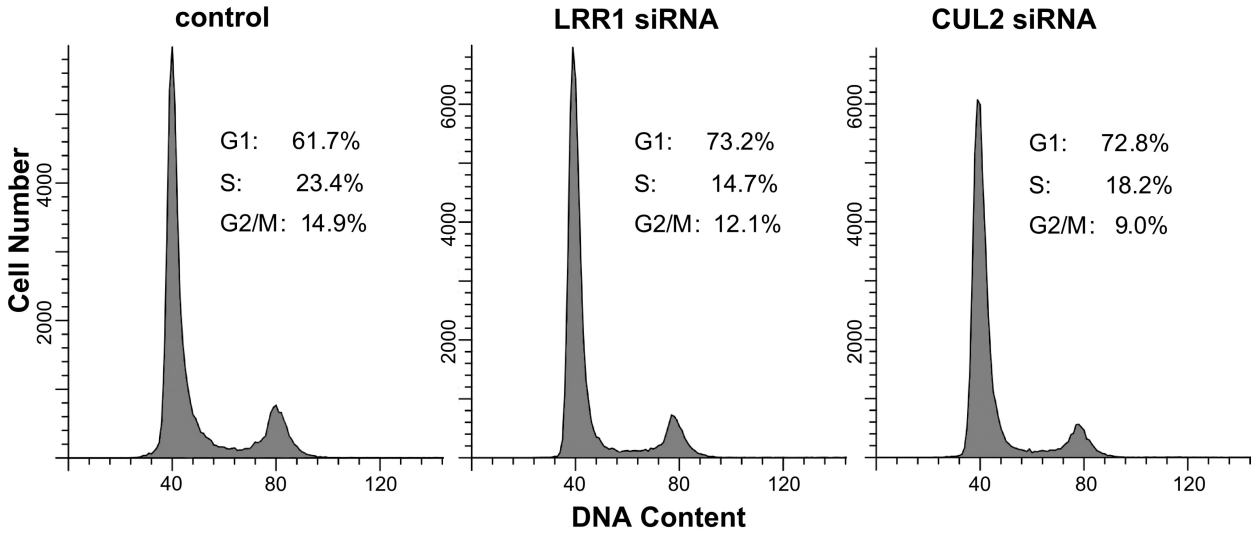

Figure S2, related to Figure 6. Flow cytometry profiles of DNA content of IMR-90 cells transfected with LRR1 or CUL2 siRNA

Cell cycle phase distributions were determined using the ModFit program. Both GFP siRNA-treated cells or untreated cells were used as controls and gave similar DNA content profiles; the data for untreated cells is presented.

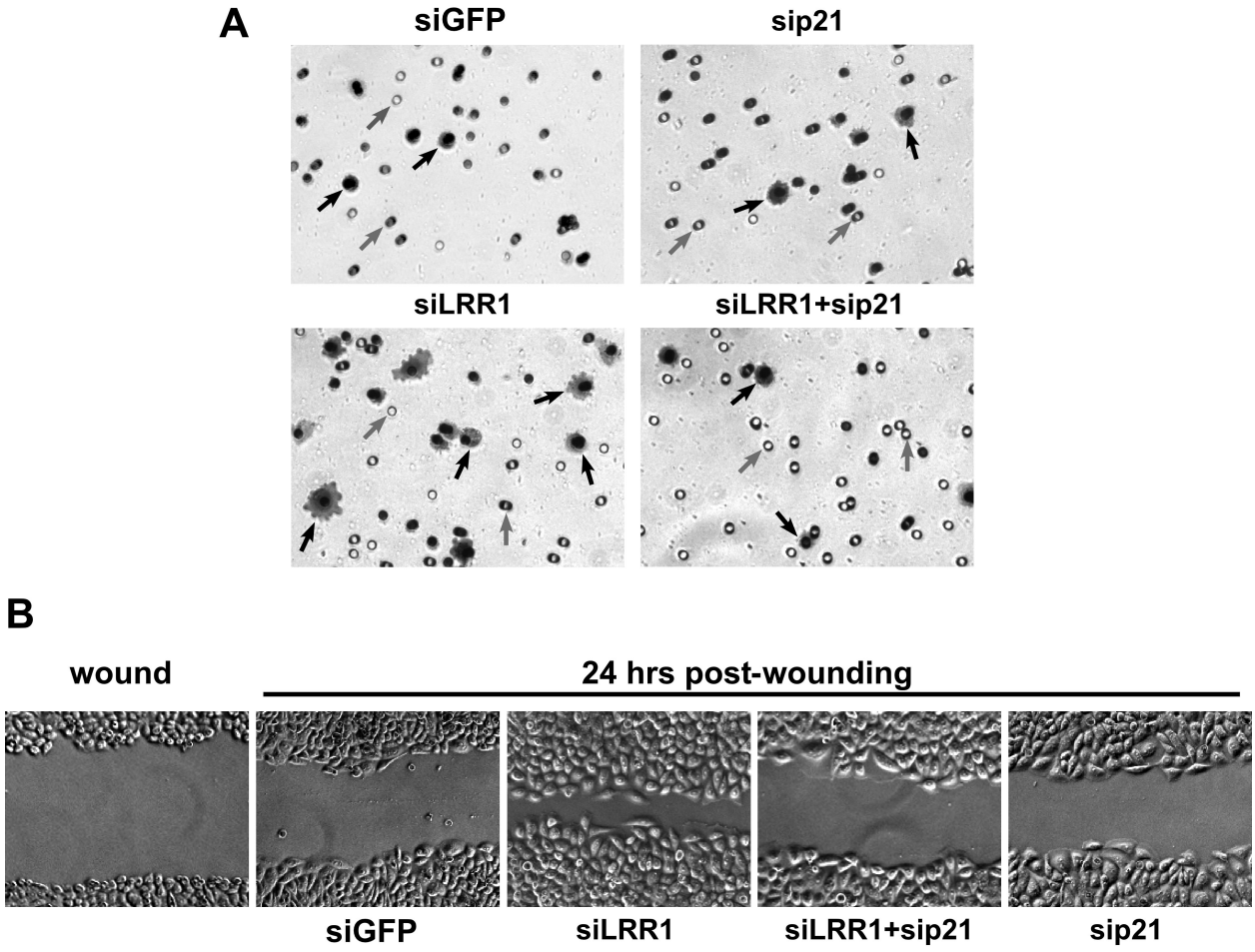

Figure S3, related to Figure 7. p21 siRNA suppresses the increased motility of HeLa cells treated with LRR1 siRNA

(A) Transwell cell migration assay. HeLa cells were transfected with siRNAs to GFP, LRR1, p21, or LRR1 + p21, and allowed to migrate across the membrane for 8 hrs. The numbers of cells that migrated across the membrane were counted in 8-10 random fields of view, in two transwells. The panels are representative images of cells that migrated across the transwell membrane (Phase contrast, 200x magnification). Note that LRR1 knockdown cells demonstrated significantly higher motility than control siGFP cells: 88 ± 11 (SD) vs. 32 ± 6 migrated cells per field of view; while the number of LRR1 + p21 double siRNA-treated cells that migrated across the membrane was low and comparable to the control: 23 ± 5. The number of p21 siRNA-treated cells that migrated was also low: 26 ± 7. SD, standard deviation. Cells are indicated by black arrows; the filter pores are indicated by gray arrows. **(B)** Wound-healing cell migration assay. Confluent HeLa cells were treated with the indicated siRNAs, followed by incubation with mitomycin C, and scraped to form a 0.8 mm wide lane lacking cells. The images are representative of 5 wounds at time 0 (wound) and at 24 hrs post-wounding healing (50x magnification). Note that the increased motility of LRR1 knockdown cells was suppressed upon treatment with double LRR1 + p21 siRNAs.

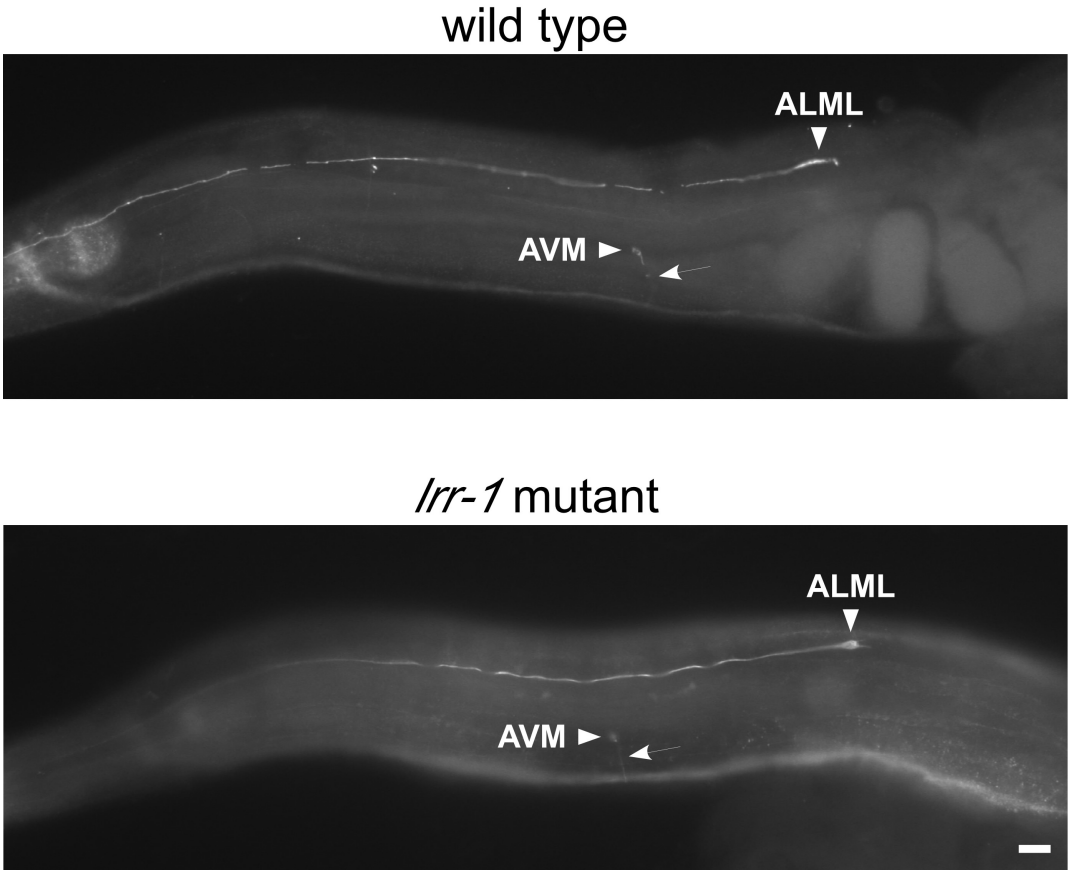

Figure S4, related to Figure 7. Touch receptor neurons in wild type and *lrr-1* mutant
Immunofluorescence micrograph of wild type and *lrr-1(tm3543)* mutant adults stained with anti-acetyl K40 α-tubulin 6-11B-1 antibody. The location of the ALML and AVM cell bodies are labeled. The axon from AVM that travels to the ventral nerve cord is labeled with a white arrow. Note that the ventral nerve cord, which also stains with the 6-11B-1 antibody, is partially out of focus. Ventral is down and anterior is to the left. Scale bar is 10 μm.

Table S1, related to Figure 6. Expression of an LRR1 construct resistant to siRNA rescues the low abundance of stress fibers in HeLa cells treated with LRR1 siRNA

siRNA	LRR1 expressed	Low stress fiber abundance (% of cells)	cell number (n)
GFP	Wild type	11.4	123
LRR1	Wild type	71.8	124
GFP	Resistant	10.3	116
LRR1	Resistant	23.2	112

‡ low stress fiber abundance: ≥60% of the cell volume lacks visible stress fibers

Table S2, related to Figure 6. Stress fiber abundance in HeLa cells upon LRR1 and double LRR1 + p21 knockdown

siRNA	Stress fiber abundance (% of cells)		cell number (n)
	high‡	low‡‡	
GFP	82.8	7.5	134
p21	89.5	4.8	105
LRR1	8.1	82.0	111
LRR1 + p21	78.0	13.6	118

‡high: stress fibers were visible over ≥70% of the cell area
‡‡low: stress fibers were visible over ≤30% of the cell area

SUPPLEMENTAL EXPERIMENTAL PROCEDURES

C. elegans strains and analysis

The following strains were used: N2 wild type, ET099 *cul-2*(*ek1*)/*unc-64*(*e246*); *ekEx19*[genomic *cul-2*(+) with a FLAG-tag sequence inserted before the *cul-2* Stop codon + pRF4 plasmid containing *rol-6*(*su1006*) + N2 genomic DNA], ET428 *lrr-1(tm3543)/mnc-1*, VC170 *cki-1(gk132)*/*mIn1*[*dpy-10(e128)*; *mIs14*], ET460 *lrr-1(tm3543)*/*mIn1*, PD4559 *ccIs4595*[*ceh-24*::GFP and pRF4], ET461 *lrr-1(tm3543)*/*mIn1*; *ccIs4595*, JR667 *unc-119(e2498::Tc1)*; *wIs51*[scm::GFP; *unc-119(+)*], ET473 *lrr-1(tm3543)*/*mIn1*; *wIs51*, ET474 *ekSi5*[*Ppie-1*::GFP::LRR-1::*tbb-2* 3'UTR]. The *Ppie-1*::GFP::LRR-1::*tbb-2* 3'UTR transgene in strain ET474 was integrated as a single copy on chromosome II using the MosSCI transposon system (Frokjaer-Jensen et al., 2008). The integration was confirmed by PCR with primers to the genomic integration loci.

To analyze GFP::LRR-1 expression in the germline, gonads were dissected from young adults in L15 media with 10% fetal bovine serum that was adjusted to 340 mOsm with sucrose. Three independent GFP::LRR-1 integrant strains gave the same germline expression pattern.

The number of vulva cells was determined by counting vulval nuclei of L4-stage larvae anesthetized with 25 mM levamisole, using a computer monitor to amplify the DIC images. The number of seam cells was determined in young adults expressing the seam cell marker scm::GFP by counting GFP-positive cells per lateral side.

The positions of vulval muscles in young adults were determined in strains expressing *ceh-24*::GFP, which is expressed in vulval muscles (Harfe and Fire, 1998). The vulval muscles derive from the division of the sex myoblasts. The two sex myoblasts are formed on opposite lateral sides of the animal during the L1 larval stage. During the L2 stage, the two sex myoblasts migrate on opposite lateral sides from the mid-posterior of the larvae to the middle of the gonad. During the L3 stage, each sex myoblast divides to produce four vulval muscles and four uterine muscles. (Sulston and Horvitz, 1977).

The migration path of the DTCs was determined by observing the shape of the gonad in young adults using DIC microscopy. During the L1-L3 stages, the DTCs migrate from the ventral midsection toward the two ends of the hermaphrodite on opposite lateral sides of the worm; at the beginning of the L4 stage, the DTCs turn dorsally, and then turn back toward the midsection along the dorsal surface (Kimble and Hirsh, 1979). The 'U' shape of each gonad arm reflects the migration path of the DTCs.

The position of the cell body and axons of five of the six touch receptor neurons (TRNs) was determined by immunofluorescence with anti-acetyl K40 α-tubulin 6-11B-1 antibody in young adults, as described (Fukushige et al., 1999). There are six touch receptor neurons: ALML, ALMR, AVM, PVM, PLML, and PLMR. ALML and ALMR migrate posteriorly in the embryo and send axons to the anterior; AVM and PVM migrate anteriorly during the larval stages and send axons toward the anterior; and PLML and PLMR send axons anteriorly (Hedgecock et al., 1987). PVM could not be reliably stained by 6-11B-1 in wild type or *lrr-1* mutants, and so was not analyzed.

Immunofluorescence in *C. elegans*

Anti-CKI-1 immunofluorescence of dissected gonads was as described (Feng et al., 1999). Immunofluorescence with anti-acetyl K40 α-tubulin (6-11B-1; 1:500) was performed using the freeze-crack method on young adults (Miller and Shakes, 1995), with 15 min fixation in

methanol and 15 min in acetone, followed by air drying, blocking in 3% BSA in PBS, and incubation with primary and secondary antibodies in 1% BSA in PBS, with intervening washes with PBST (PBS + 0.2% Tween-20). A Zeiss Axioskop microscope was used for DIC and immunofluorescence microscopy. A Hamamatsu ORCA-ER digital camera run by Openlab 5.0.2 software (Improvision) was used to capture images. Matched immunofluorescence images were taken at the same exposure and processed identically using Adobe Photoshop software. Quantitation of immunofluorescence signal was performed with Adobe Photoshop, version CS2.

Affinity purification from *C. elegans* extract

Affinity purification of *C. elegans* CUL-2::FLAG associated proteins was performed as previously described (Starostina et al., 2007). Late L4 larvae or young adults of the strain ET099, which expresses CUL-2::FLAG, were collected, purified by flotation on 30% sucrose and frozen at -80^{o}C, then ground in liquid nitrogen, followed by suspension in Lysis buffer: 50 mM HEPES, pH7.8; 300 mM NaCl; 10% glycerol; 0.2% Triton X-100; 2 mM DTT; 1 mM EDTA; and protease inhibitor cocktail (Roche). The extract was clarified by consecutive low speed (1,500xg 5 min) and high speed (100,000xg 40 min) centrifugations and incubated for 2 hrs at 4^{o}C with anti-FLAG M2 antibody coupled to agarose beads (Sigma) in the presence of 200 mM NaCl/Lysis buffer. After washing with the latter buffer, bound proteins were eluted with 0.4 mg/ml FLAG peptide (Sigma) in Elution buffer: 20 mM HEPES, pH7.8; 150 mM KCl; 15% glycerol; 0.05% NP-40; 2 mM DDT; 1 mM EDTA, and protease inhibitor cocktail. As a control for the specificity of the affinity purification, we used wild-type animals (not expressing FLAG-tagged CUL-2). Proteins that were identified in the control affinity purification were considered non-specific. The eluates were resolved on NuPAGE 4-12% Bis-Tris gels, and stained with SYPRO Ruby (Molecular Probes) or Coomassie R-250 (Sigma) and used for MALDI-TOF MS identification of individual protein bands (University of Georgia Proteomics Facility), or for LC-MS/MS (with J.-m. Lim and L. Wells). In separate experiments, the eluates were analyzed by trypsin digestion in solution followed by LC-MS/MS using a Thermo Finnigan LTQ mass spectrometer with Nanoflow HPLC and nanospray capability. LC-MS/MS data was analyzed with Bioworks/Turbosequest software.

In our initial affinity purification, LRR-1 was identified as a single peptide, along with the known SRSs ZYG-11 (1 peptide), ZER-1 (4 peptides), and FEM-1 (7 peptides). None of these proteins were identified in the control sample. In two subsequent independent CUL-2::FLAG affinity purification experiments, LRR-1 was identified by 5 and 6 peptides, while the other known SRSs were also identified by a higher number of peptides: ZYG-11 (5 and 4 peptides), ZER-1 (27 and 33 peptides), and FEM-1 (19 and 19 peptides). We have previously described the identification of the core CRL2 components Rbx1 (RBX-1), Elongin C (ELC-1), and Elongin B (ELB-1) in *C. elegans* using affinity purification of CUL-2::FLAG coupled to LC-MS/MS (Starostina et al., 2007).

Expression constructs

C. elegans full-length *lrr-1* and *cki-1* cDNA sequences were amplified from the RB1 cDNA library (Barstead and Waterston, 1989). cDNAs encoding human LRR1, p21, and ubiquitin were obtained from the following plasmids: FLAG-LRR1/pCDNA3, 3xFLAG-LRR1/pCDNA3/Puro, p21/pCS2, and HA-Ub/pCMV, which were gifts from B. S. Kwon, K. I. Nakayama, B. E. Clurman and Y. Xiong, respectively. cDNAs, either untagged or fused to epitope tags, were cloned into pCMV-Tag2 (Stratagene), pEGFPN1 (Invitrogen), pGEX-2T (Amersham), or pET-15b (Novagen) vectors. In the pEGFPN1 vector, the EGFP sequence was removed. The following constructs were created: FLAG-LRR-1/pCMV-Tag2; LRR-1/pET-15b; LRR-1/pGEX-2T; CKI-1/pGEX-2T; HSV-LRR-1/pEGFPN1; and VSVG-CKI-1/pEGFPN1. FLAG-

CKI-1/pCMV-Tag2, p21/pCS3-MT, p21/pCDNA3, and PIP-box mutant p21/pCDNA3 were described in our earlier work (Kim et al., 2008). For the FLAG-LRR1Δ construct, a deletion of the VHL-box motif (amino acid residues 320 through 356) was made by overlapping PCR mutagenesis (Mikaelian and Sergeant, 1992). The FLAG-LRR1/pCDNA3 rescue construct (resistant to LRR1 siRNA #1) was created by overlapping PCR mutagenesis to introduce 5 silent mutations (indicated in lower case) in the region of LRR1 coding sequence targeted by the siRNA: GAAgGCtACcGTcCGcTTA.

siRNA sequences

We used LRR1 ON-TARGETplus siRNAs from Dharmacon as a pool of four siRNAs or as individual siRNAs; the sequences are as follows (overhanging bases are in lowercase): GAAAGCCACUGUUCGGUUAuu (#1); GUGGAUAUCUGUCUAAGUAuu (#2); ACACUGUGGUCUUAGUAGAuu (#3); and GCGUCAAAUUGGAGUAAGGuu (#4). The following siRNAs were generated by Invitrogen: siGFP, GCUGACCCUGAAGUUCAUCUGdTdT; siCUL2, GAACUGCUUGCUAAGUACUGUdTdT (sequence from(Kamura et al., 2004)); sip21, CUUCGACUUUGUCACCGAGdTdT; and siSkp2, GGAUGUGACUGGUCGGUUGdTdT.

Antibodies

The following mouse monoclonal antibodies were used: anti-p21 (Upstate Biotechnologies), anti-CUL2 (BD Transduction Laboratories); anti-α-tubulin (DM1A, Sigma); anti-actin (C4, ICN); anti-FLAG (M2, Sigma); anti-nuclear pore complex (Mab414, Covance); anti-PARP-1 (C-2-10, Calbiochem); anti-acetyl K40 α-tubulin (6-11B-1); anti-HA.11 (Covance); anti-VSV-G (P5D4, Sigma); anti-HSV (Novagene); and anti-Myc (9E10, Covance). The following rabbit polyclonal antibodies were used: anti-CKI-1(Feng et al., 1999); anti-human CUL2 (ZYMED Laboratories); anti-p57 (Upstate Biotechnologies); anti-p27 (Upstate Biotechnologies); anti-Skp2 (H345, Santa Cruz Biotechnologies); anti-cofilin (Cell Signaling); anti-phospho-cofilin (Ser3) (Cell Signaling); anti-HA (ab9110, Abcam); anti-FLAG (Sigma); anti-HSV (GenScript USA INC); and anti-VSV-G (Bethyl). Secondary antibodies were goat anti-rabbit or anti-mouse Rhodamine-conjugated antibodies (Cappel), and goat anti-mouse Alexa-Fluor 488 (Molecular Probes). Rhodamine-conjugated phalloidin was used for F-actin staining. DNA was stained with 1 μg/ml Hoechst 33258 (Sigma).

Mammalian cell culture and DNA transfection

HeLa and HEK293T cells were grown in Dulbecco's modified Eagle's medium (DMEM) (HyClone), T98-G and IMR-90 cells were grown in Minimum Essential Medium (GIBCO-BRL), supplemented with 10% fetal bovine serum (FBS) (HyClone). Expression constructs were transiently transfected into HEK293T, or HeLa cells using Lipofectamine 2000 (Invitrogen) in accordance with the manufacturer's instructions. To isolate HeLa cell lines stably expressing 3xFLAG-LRR1, cells were transfected with 3xFLAG-LRR1/pcDNA3/Puro (Kamura et al., 2004) and selected with 0.7 μg/ml of puromycin (Sigma).

Cell fractionation

Cell fractionation was performed essentially as in Sarcinella et al., 2007 (Sarcinella et al., 2007). Briefly, the cytosolic fraction was prepared by short, 5-min lysis of the cells with 0.2% Triton X-100 in one volume of cold buffer A (20 mM HEPES, pH7.8; 10 mM KCl, 1.5 mM $MgCl_2$, 0.34 M sucrose, and 10% glycerol) supplemented with 1 mM DTT,
1 mM EDTA, 10 mM iodoacetamide, and 15 μM MG132. After low-speed pelleting of nuclei, the cytosolic fraction was separated and boiled with 1% SDS. Nuclei were washed in buffer A without detergent, pelleted and boiled in one volume of Buffer A containing 1% SDS. A sample

of whole cell lysate (Total) was prepared by boiling the same amount of cells in two volumes of buffer A with 1% SDS. Equal volumes of the samples were analyzed by western blot.

***in vitro* binding experiments**

GST, GST-fused CKI-1, and GST-LRR-1 were expressed in *E. coli* strain Origami B(DE3) (Novagen) and induced with 0.4 mM IPTG. Bacteria were disrupted by sonication in Binding buffer: 50 mM Tris, pH 7.4; 500 mM NaCl; 0.05% NP-40; 2 mM DTT; 1 mM EDTA; and protease inhibitor cocktail. Pre-cleared supernatant (2,500xg, 20 min centrifugation followed by filtering through a 1 µm pore PVDF membrane [Millipore]) was incubated with Glutathione Sepharose 4 Fast Flow beads (GE Healthcare) for 1 hr at room temperature. The beads with immobilized GST-fusion protein or GST were washed in Binding buffer and then incubated for 1 hr at room temperature in Binding buffer with ^{35}S-labeled protein that was translated with the TnT Coupled Wheat Germ Extract systems (Promega) with T7 or T3 RNA polymerase using the *lrr-1*/pET15b, or *cki-1*/pCMV plasmids. After washing with Binding buffer, beads were boiled in SDS sample buffer and analyzed by SDS-PAGE and autoradiography.

SUPPLEMENTAL REFERENCES

Barstead, R.J., and Waterston, R.H. (1989). The basal component of the nematode dense-body is vinculin. J Biol Chem *264*, 10177-10185.

Frokjaer-Jensen, C., Davis, M.W., Hopkins, C.E., Newman, B.J., Thummel, J.M., Olesen, S.P., Grunnet, M., and Jorgensen, E.M. (2008). Single-copy insertion of transgenes in Caenorhabditis elegans. Nat Genet *40*, 1375-1383.

Fukushige, T., Siddiqui, Z.K., Chou, M., Culotti, J.G., Gogonea, C.B., Siddiqui, S.S., and Hamelin, M. (1999). MEC-12, an alpha-tubulin required for touch sensitivity in C. elegans. J Cell Sci *112 (Pt 3)*, 395-403.

Harfe, B.D., and Fire, A. (1998). Muscle and nerve-specific regulation of a novel NK-2 class homeodomain factor in Caenorhabditis elegans. Development *125*, 421-429.

Mikaelian, I., and Sergeant, A. (1992). A general and fast method to generate multiple site directed mutations. Nucleic Acids Res *20*, 376.

Miller, D.M., and Shakes, D.C. (1995). Immunofluorescence microscopy. Methods Cell Biol *48*, 365-394.

Sarcinella, E., Zuzarte, P.C., Lau, P.N., Draker, R., and Cheung, P. (2007). Monoubiquitylation of H2A.Z distinguishes its association with euchromatin or facultative heterochromatin. Mol Cell Biol *27*, 6457-6468.

Sulston, J.E., and Horvitz, H.R. (1977). Post-embryonic cell lineages of the nematode, Caenorhabditis elegans. Dev Biol *56*, 110-156.